

Supplementary Information

Photo-Kelvin Probe Force Microscopy for Photocatalytic Performance Characterization of Single Filament of TiO₂ Nanofiber Photocatalysts

Ming-Chung Wu,^{a*} Hseuh-Chung Liao,^b Yu-Cheng Cho,^c Géza Tóth,^d Yang-Fang Chen,^c Wei-Fang Su,^b
and Krisztián Kordás^{d,e}

^a Department of Chemical and Materials Engineering, Chang Gung University, Taoyuan 33302, Taiwan
Tel: +886 3 2118800 ext.3545; E-mail: mingchungwu@mail.cgu.edu.tw

^b Department of Materials Science and Engineering, National Taiwan University, Taipei 10617, Taiwan

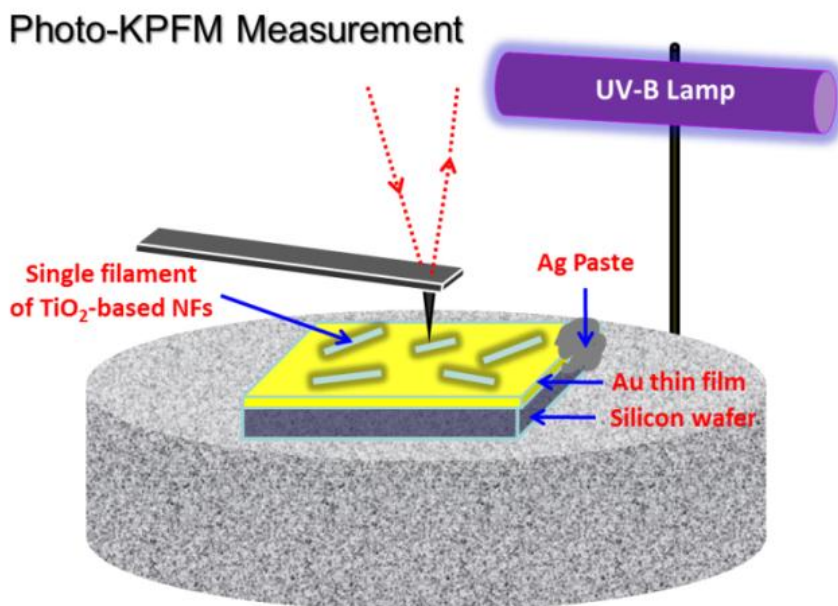
^c Department of Physics, National Taiwan University, Taipei 10617, Taiwan

^d Microelectronics and Materials Physics Laboratories, Department of Electrical and Information Engineering, University of Oulu, Oulu FIN-90014, Finland

^e Technical Chemistry, Department of Chemistry, Chemical-Biological Center, Umeå University, SE-901 87 Umeå, Sweden

15

The surface potential mapping is measured by a Kelvin probe force microscope (Digital Instruments, Nanoscopes III) at room temperature. Conductive tips were used to obtain the surface potentials. An n-type silicon cantilever (Nanosensors), which is soft (average force constant ~2.8 N/m) and with resonance frequencies of 75 kHz in average, is coated with chromium and Platinum-Iridium5 alloy as buffering layer and conductive layer respectively. The substrate (100 nm thick gold coated on the silicon wafer) with TiO₂ nanofibers dispersed on top was attached on to the KPFM metal holder. Then, the silver paste was applied to ground the substrate (gold) to the metal holder. The KPFM was subsequently performed after drying the silver paste under vacuum. The surface potential distribution of TiO₂ nanofibers can be mapped either in dark or under illumination by a UV-B lamp (Sankyo Denki, G8T5E, 8 W). Fig. S1 shows the schematic illustration of this photo-KPFM measurement. The surface potential difference between dark and illumination ($SP_{\text{dark}} - SP_{\text{light}}$) is defined as the surface potential shift (SP shift).



30

Fig. S1 Schematic illustration of photo-KPFM measurement.

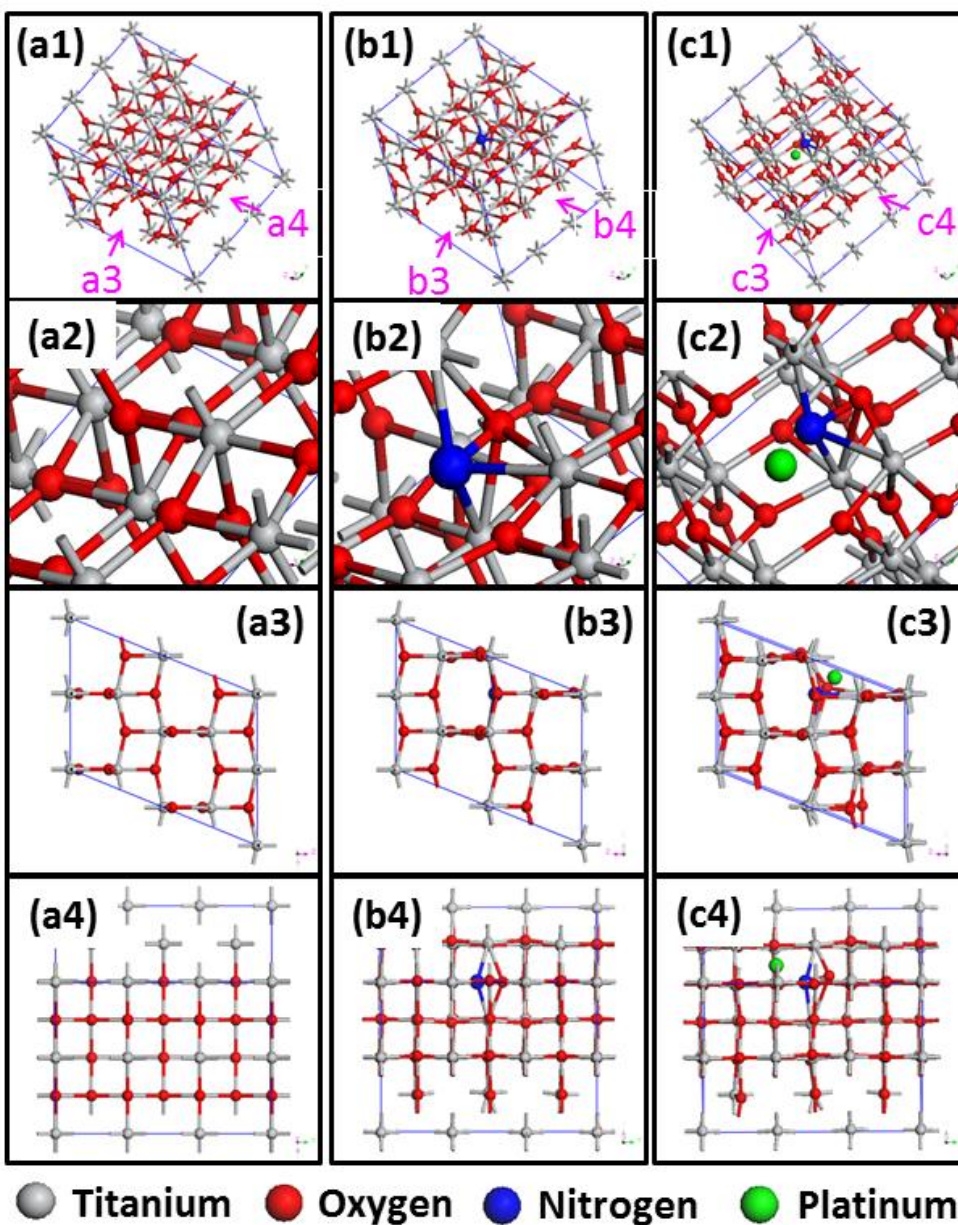


Fig. S2. Structures of TiO_2 NFs (a), N- TiO_2 NFs (b), and N- TiO_2 -Pt NFs (c), used in this study are demonstrated; all models are made of $(2 \times 3 \times 1)$ anatase TiO_2 supercell. (a1, b1, c1) The general view of the structures is given with nitrogen atoms indicated in blue and platinum atom indicated in green. (a2, b2, c2) Large magnification images are showed and to compare the main difference between these three structures. In interstitial doping, nitrogen is in the same site with oxygen and forms four bonds with its neighboring atoms (three with titanium one with oxygen). (a3, b3, c3) and (a4, b4, c4) are images observed from different viewpoints, and the viewpoints we adopted are showed with arrows in (a1, b1, c1). The distortion in lattice structure caused by impurities are clearly revealed in (a3, b3, c3) and (a4, b4, c4).

10

Table S1. Theoretical band gap for TiO_2 -based materials

Material	Band gap (eV)
Anatase TiO_2	2.441
N- TiO_2	1.514
N- TiO_2 -Pt	1.385

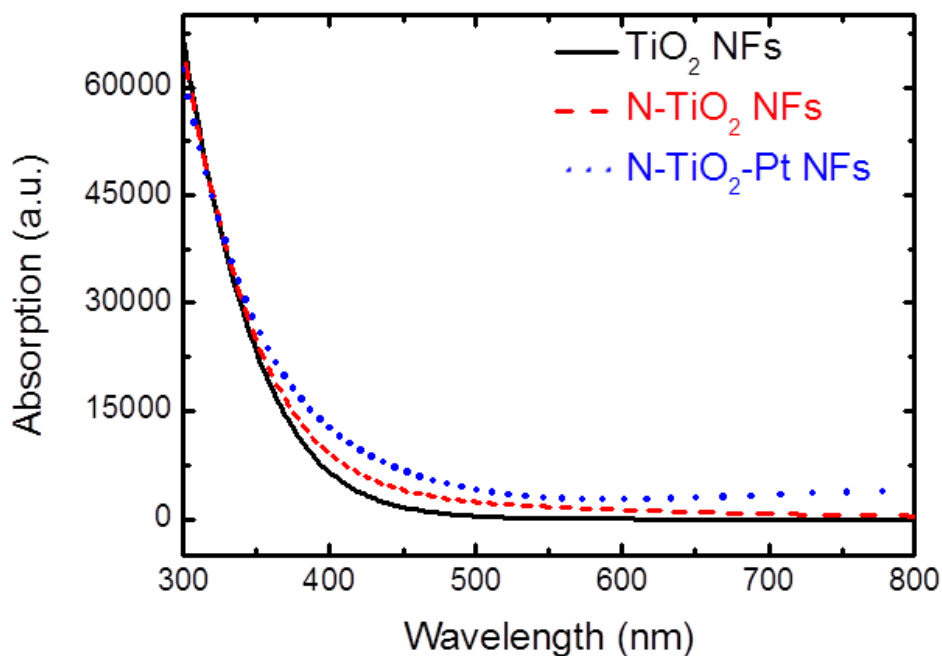


Fig. S3. Theoretical absorption spectrum of TiO_2 , N-TiO_2 NFs and $\text{N-TiO}_2\text{-Pt}$ NFs. Scissor operator of 0.759 eV provided in Material Studios is used to correct the underestimation in band gap when predicting absorption spectrum. Red shift can be observed in both N-TiO_2 NFs and $\text{N-TiO}_2\text{-Pt}$ NFs and the shifting effect is stronger after Pt decoration.

5

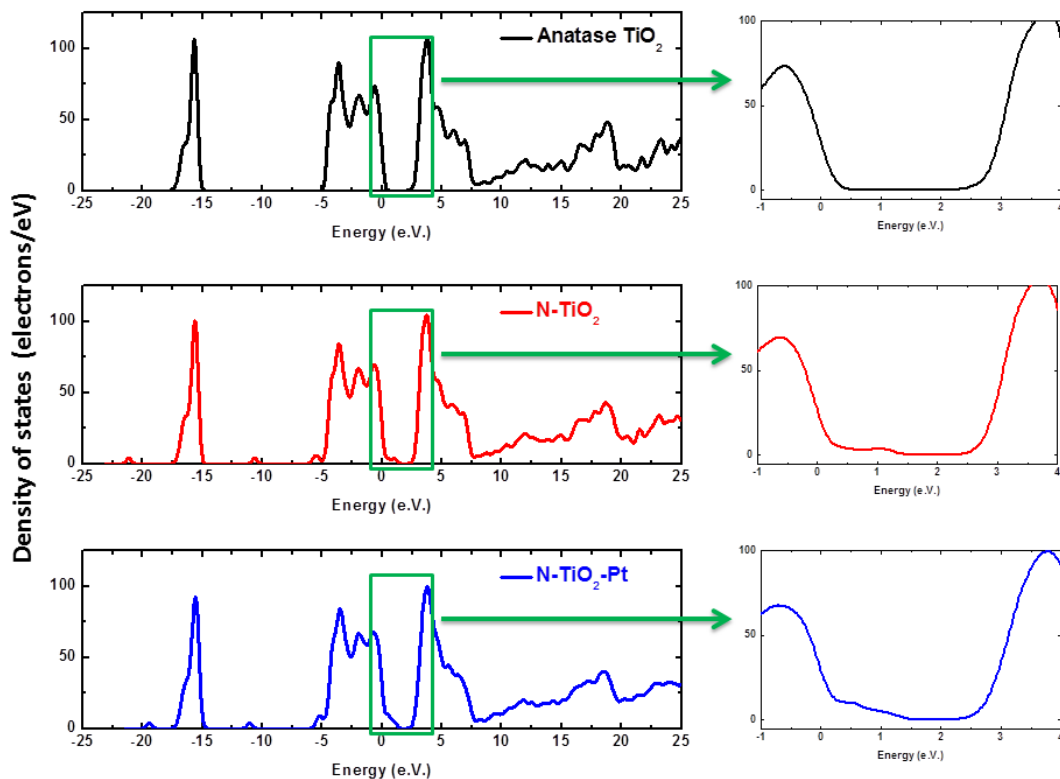


Fig. S4. Density of states of TiO_2 , N-TiO_2 and $\text{N-TiO}_2\text{-Pt}$. States generated by impurities can be observed in both N-TiO_2 and $\text{N-TiO}_2\text{-Pt}$ with energy level slightly surpass valence band. These states are more remarkable in $\text{N-TiO}_2\text{-Pt}$ and the narrowing band gap can also be observed due to the generation of impurity states.

10